



## ARTICLE

# PV Solar Yield Applicable Simulator Based on Free Irradiance Data Source: Applied Comprehensive Tool for Solar Engineers

Ahmed Mohamed Ragab<sup>1,\*</sup>, Abdelhalim Abdelnaby Zekry<sup>2</sup> and Ashraf Yahia Hassan<sup>1</sup>

<sup>1</sup>Faculty of Engineering, Communication Section, Benha University, Benha, 13511, Egypt

<sup>2</sup>Faculty of Engineering, Communication Section, Ain Shams University, Cairo, 11566, Egypt

\*Corresponding Author: Ahmed Mohamed Ragab. Email: ahmed.ragab17@beng.bu.edu.eg; ahammob@yahoo.com

Received: 05 September 2022 Accepted: 24 November 2022

## ABSTRACT

Accurate PV system simulators are implemented with expensive software platforms using paid irradiance data. The main purpose of this paper is to develop and validate a PV system simulator, beginning with a solar cell parameter extraction model, then test and validate long-term Irradiance data using free online source (Typical Meteorological Year TMY in (PVGIS) European website), and finally building full solar generator simulator to run in working real conditions. Comparing results with Accurate Paid PV simulators (which use the Muneer model) showed good accuracy of the proposed simulator. Work flow starts with the Irradiance model's data processing, then solar cell 5 parameters model data processing (to extract cell parameters), and finally full system simulator. MATLAB coding programs in real working conditions are used for simulation. Results of solar cell parameter extraction show 99.6% to 99.99% matching with data sheet and cell performance under standard test conditions. System model simulation output shows 8% less yearly generated energy compared to the PVGIS 2022 long-term simulation (hourly basis (one-year time)). This is due to incident energy variations (between the years 2016 and 2022) of 4.02%. The novelty of the algorithm is the methodology, as it tests irradiance data on an hourly basis and validates results for a whole continuous year. Also, the 5-parameter solar cell model is used to be validated in long term analysis, not only STC conditions and could be applied on any PV solar cell. The algorithm and block diagram used are scalable, modular, and interchangeable with similar models to be tested. This simulator could test several methods and models in solar pv technology.

## KEYWORDS

Photovoltaics; solar systems; solar cell parameters extraction; solar simulation model; irradiance models; solar yield; long term analysis

## Nomenclature

Parameter	Description of the Parameter
$a$	Ideality factor of the solar cell
$a_{am,j}$	A string of constants for airmass modifier equation
$A_M$	Module azimuth [°]
$A_M$	Module altitude [°]
$A_S$	Sun azimuth [°]



This work is licensed under a Creative Commons Attribution 4.0 International License, which permits unrestricted use, distribution, and reproduction in any medium, provided the original work is properly cited.

$a_s$	Sun altitude [°]
$AOI$ or $(\theta_z)$	Angle of incidence [°]
$DHI$	Diffuse horizontal irradiance [W/m <sup>2</sup> ]
$DNI$	Direct normal irradiance [W/m <sup>2</sup> ]
$DNI_{EX}$	Hourly extraterrestrial solar radiation on horizontal surface empirical formula [W/m <sup>2</sup> ]
$E_g$	Band gap energy of the semiconductor [ev]
	Energy [Wh]
$SH$	Equivalent sun hours [h]
	Yearly electricity yield [Wh/year. KW <sub>P</sub> ]
$FF$	Fill factor [–]
$G$	Surface irradiance of the cell [W/m <sup>2</sup> ]
$G_{M-AM}^{tot} (i)$	Total irradiance on module affected by airmass modifier [W/m <sup>2</sup> ]
$G_M^{alb}$	Albedo irradiance [W/m <sup>2</sup> ]
$G_M^{dif}$	Diffused irradiance [W/m <sup>2</sup> ]
$G_M^{dir}$	Direct normal irradiance [W/m <sup>2</sup> ]
$G_M^{tot}$	Total irradiance on square meter of the panel [W/m <sup>2</sup> ]
$G_{STC}$	Irradiance under STC (=1000 W/m <sup>2</sup> )
$GHI$	Global horizontal irradiance [W/m <sup>2</sup> ]
$i$	Hourly index of the airmass modifier
$I_0$	Diode saturation current [A]
$I_{S(STC)}$	Nominal saturation current [A]
$I_{SC}$	Short circuit current of the solar cell [A]
$I_{SC(STC)}$	Short circuit current per cell at STC [A]
$I_{mp}$	Max. power point current [A]
$k_B$	Boltzmann's constant [J · K <sup>-1</sup> ]
$K_l$	Temperature coefficient of short circuit current [%/°C]
$K_V$	Temperature coefficient of open-circuit voltage [%/°C]
$M (i)$	Airmass modifier
$n$	Diode ideality factor
$P_{max}$	Maximum output power [W]
$P$	Power [W]
$PF$	Power factor
$R_s$	Series resistance of the solar cell [Ω]
$R_{sh}$ or $R_b$	Shunt resistance of the solar cell [Ω]
$R$	Actual sun-Earth distance [m]
$SVF$	Sky view factor
$S$	Extraterrestrial radiation on horizontal plan [Wh/m <sup>2</sup> ]
$T$	Absolute temperature in Kelvin [K]
$V_T$	Thermal voltage of the diode [V]
$V_{oc}$	Open circuit voltage of the solar cell [V]
$V_{mp}$	Max. Power point voltage [V]
$\alpha_{gnd}$	Albedo coefficient
$\theta_M$	Module tilt angel in degrees [°]
$N$	Number of modules [–]
<b>Abbreviation</b>	<b>Description of the Abbreviation</b>
<i>BSRN</i>	Baseline Surface Radiation Network
<i>DAQ system</i>	Data acquisition system in LabVIEW application

<i>DC</i>	Direct current
<i>EGP</i>	Egyptian Pound
<i>IV</i>	Current voltage curve
<i>KW<sub>p</sub></i>	Kilo watt peak system size
<i>MATLAB</i>	Matrix laboratory
<i>NAN</i>	North African Nations
<i>PV</i>	Photovoltaic
<i>PVGIS</i>	Photovoltaic Geographical Information System of European Union
<i>PVSYST</i>	Photovoltaic software PC package
<i>STC</i>	Standard test conditions at which ( $T_{STC} = 25^{\circ}\text{C}$ )
<i>SWPS</i>	Solar water pumping system
<i>TMY</i>	A typical meteorological year
<i>LCOE</i>	Levelized cost of electricity [€/KWh]

## 1 Introduction

Most North African nations (NAN), especially Egypt, are suffering from water scarcity Abdelhaleem et al. [1]. In Adun et al. [2] study, the energy-water entanglement in the NAN region was reviewed, it showed that there was a very deep dependence on energy for fresh water. Their study mentioned that in Libya and Egypt, 14% of the total fuel consumption is due to groundwater pumping and wastewater treatment. This validates that the energy-water entanglement is a key area for concern in the NAN region. As example, depending on fossil fuel, which has high carbon emissions and high prices for pumping or treating water in the agricultural sector, is less cost effective than solar energy. According to latest statistics, diesel fuel in Egypt has reached 6.75 EGP (0.43 \$) of an increase of more than 6 times in just 10 years. The PV solar pumping irrigation system has been widely used in Egypt. A study of the PV pumping system Sontake et al. [3] (considering a 10 feddan irrigation system of nominal power of 7 KW<sub>p</sub> and a life time cycle of 20 years for the pv solar system and 10 years for the diesel pumping system) proves that PV pumping system saves more than 30% cost less than diesel generator pumping system cost. Parvaresh Rizi et al. [4,5] presented financial comparative study of solar and regular irrigation pumps which shows the carbon dioxide emission reduction and cost effectiveness of solar pumping systems., On grid systems is another example of solar energy utilization importance. According to the Egyptian government, the solar energy generation capacities could be extended by 3500 MW by the end of 2027, Shouman [6]. After inference, the importance of solar PV generation, solar PV system design and analysis will be discussed in the next paragraph. The first stage in designing any PV solar system (or solar generator) is to determine the load profile, and predict solar energy yield. Calculations are done to estimate the nominal power of the pv generator based on average equivalent sun hours (ESH) in any location. Using an unsuitable PV model or Irradiance model will lead to system errors, which will affect the predicted energy output of the system. Consequently, it will lead to generated energy shortage, design failure, and loss of capital investment. The design and simulation models of solar generator (to predict solar system performance) account for a good Irradiance model, PV cell/array model, Irradiance database (preferably a free source), and lastly, location coordinates, since all calculations related to the specific location of the system. In this paper, we will discuss solar generator design and analysis, in addition to practical working conditions to determine the solar energy yield all over the year. In the system model, all kinds of losses are based on component efficiency and must be considered carefully. Literature had many irradiance models which determine diffuse, direct, and global irradiance. The two big categories of diffuse Irradiance models are parametric models and Decomposition models. In parametric models Gueymard [7], the necessary

parameters are needed to determine hourly diffuse radiation like atmospheric turbidity, fractional sunshine, cloud cover, and perceptible water content. Yadav et al. [8] used the parametric model to determine diffuse radiation. On the other hand, Decomposition models use only global horizontal radiation data to get the diffuse radiation, using the clear sky index Kumar et al. [9]. A model for determining Diffuse irradiance based on measured data and clear sky index in the USA is presented Liu et al. [10]. In the wider picture, global solar radiation, which is the total radiation incident on an inclined plane, consists of 3 components: beam radiation, reflected radiation, and diffuse radiation. There are two main categorized methods: (a) Isotropic models, Liu and Jordan's Model [11]. (b) Anisotropic models, Temps and Coulson's model [12], Hay and Davies model [13]. Reindl model [14], Klucher model [15], Perez model [16], Muneer model [17]. The difference between isotropic and anisotropic models is that the first considers the diffuse radiation component to be uniformly distributed in the sky, while the most complex latter model considers the sun disk, circumsolar, and horizon brightening radiation. A very good review paper considering most famous irradiance models and good recommendations for using best of them [18]. The second step (level) for making a successful solar generator model, is to use cell model/array models. The most popular models are the 4-parameter model Chenni et al. [19], the 5-parameter model (one diode model), and the two-diode model. The one diode model has very good accuracy and less complications than the 2-diode model [20]. Thus, the one diode model will be used in this study. The most important aspect for using this model is to determine the value of the 5 parameters, which are the ideality factor ( $a$  or  $n$ ), the series resistant ( $R_s$ ), the parallel resistant ( $R_{sh}$ ), the saturation current of the diode ( $I_o$ ), and lastly the photo or light current ( $I_{ph}$ ). There are two main categorized methods to determine the 5 parameters: numerical methods, and analytical methods. In the numerical model as the equation of the solar cell is a transcendent equation and parameters  $R_s$ ,  $R_{sh}$  (or  $R_b$ ),  $n$  cannot be separated (due to the presence of an exponential term). A mathematical solution based on the Lambert W-function Ding et al. [21] was used. It explicitly extracts values of the solar cell parameters using Matlab coding. Cubas et al. [22] used the same Lambert function approach to determine the 5 parameters, while in Chenni et al. [19], 4 parameter model and bisection method with upper and lower limits of  $R_s$  is used, it extracts the 4 parameters using an iteration routine, Sera et al. [23] used 5 parameter model along with the Newton-Raphson or Bisection method. All of these numerical methods show good accuracy and validation procedures in STC conditions (standard test conditions). There proved a very small difference between the data sheet and the method, which resulted mostly in STC conditions. In the second methodology an analytic approach to determine the 5 parameters value is used, Cubas et al. [24] used an analytic approach to extract the value of the ideality factor,  $R_s$ , and  $R_b$ . The approach depends on neglecting the effect or weight of some parameters compared to others in certain equations. Zekry et al. [25] used two methods to determine the 5 parameters of the solar cell, the first method was executed by initiating the ideality factor while the second method initiating the shunt resistance STC value guided by the IV curve. Simulation was conducted using Simulink and PSpice. Although the previous efforts of determining the solar cell parameters and extracting them to a good accuracy, all the analyses were done on STC or a small period of time not using an extended time database (long analysis period is at least one year), Sahbel et al. [26] experimentally evaluated the performance of PV cell/module using DAQ system in LabVIEW, Zekry et al. [27] showed the importance of true working conditions on solar water pumping system (SWPS) as an example of solar generation system.

Modeling and testing of a solar generator at STC or during a short-term simulation period will not account for a large number of effects and variances that will dramatically affect the expected energy performance. The purpose of this literature review is to explain various models used individually in modeling PV solar system parts, however, none of those studies integrate all the models with all its

representative equations to evaluate long term operation performance, which lead us to the significance of this proposal, the main novelty of this paper could be summarized as follows:

- Processing and validating free typical meteorological year (TMY) raw Irradiance data (TMY is a set of meteorological data with data values for every hour in a year for a given geographical location. The data is selected from hourly data over a longer time period, normally 10 years or more), by calculating the global horizontal irradiance (GHI) in plan radiation using two irradiance models, then, comparing it with a GHI output of 2022 paid platform (novelty is the validation of the database available on the EU site using the proposed method under working conditions).
- Validating methodology of calculating the airmass effect on the long term in plan radiation using coding in MATLAB.
- Using and validating analytic approach to extract solar cell parameters in STC proving 99.9% matching, depending on these parameters, using panel model in PV solar generator under real working conditions for a whole year, and hourly yield data validation compared to (photovoltaic geographical information system of European union) PVGIS results.
- Integrating all models (solar irradiance model results (long term GHI) and solar panel model based on extracted parameters) in solar generator simulation model, then coding all representative equation in MATLAB to generate hourly, daily, monthly and yearly basis solar yield. This result resolution and detailed analysis is not available in PVGIS site.
- Validating PV system energy yield from this work compared to energy yield from PVGIS platform 2022.
- Solar generator model proposed as a free tool for solar engineers to estimate system yield shows 8% less yearly generated energy compared to the PVGIS 2022 long-term simulation (hourly, daily and weekly basis generation analysis in PVGIS tool is not available).

The main contribution of this paper is to present solar generation result for a nominal power system using a novel solar simulator composed of integrated models one after another, the proposed system analyses solar generated energy hourly basis for one year. The use of this system allows engineers to do a much deeper analysis of solar yield of any system. Any brand of PV panels available in the market could be tested and analyzed for parameter extraction using proposed methodology. Other advantage over PVGIS tool that, while it uses one model (Muneer model) any model could be plugged in the proposed system architecture to be tested (2 models are tested actually). The parameters extraction of any solar cell could be done and compared with manufacturer data sheet while is not available in PVGIS platform. While PVGIS gives yield results in monthly basis the proposed system gives results and analysis in hourly-daily-weekly-monthly and finally yearly basis. To determine the reliability of the proposed system, output is compared to the only available monthly solar yield of modern online simulator PVGIS. Each step is carefully tested under actual working conditions. Final results show identical performance in the first level with data sheet results, second level (in plan GHI) shows 4.02%. The difference compared to 2022 PVGIS results (using data available up to 2016). The novelty of this system is the ability of long-term simulation for PV system yield under daily working conditions, and ability of prediction of all parameter beginning of cell level.

## 2 Data and Methodology

Fig. 1 shows the location which is used to simulate data is in Egypt, Monofya governorate, Ashmon village. The coordinates in Latitude/Longitude are: 30.299, 30.987. The weather conditions



are sunny most of the year, although Irradiance decrease in winter season. Two system sizes will be simulated, the first is normalized to 1 KW<sub>p</sub> system, while the second is 8.25 KW<sub>p</sub> system.

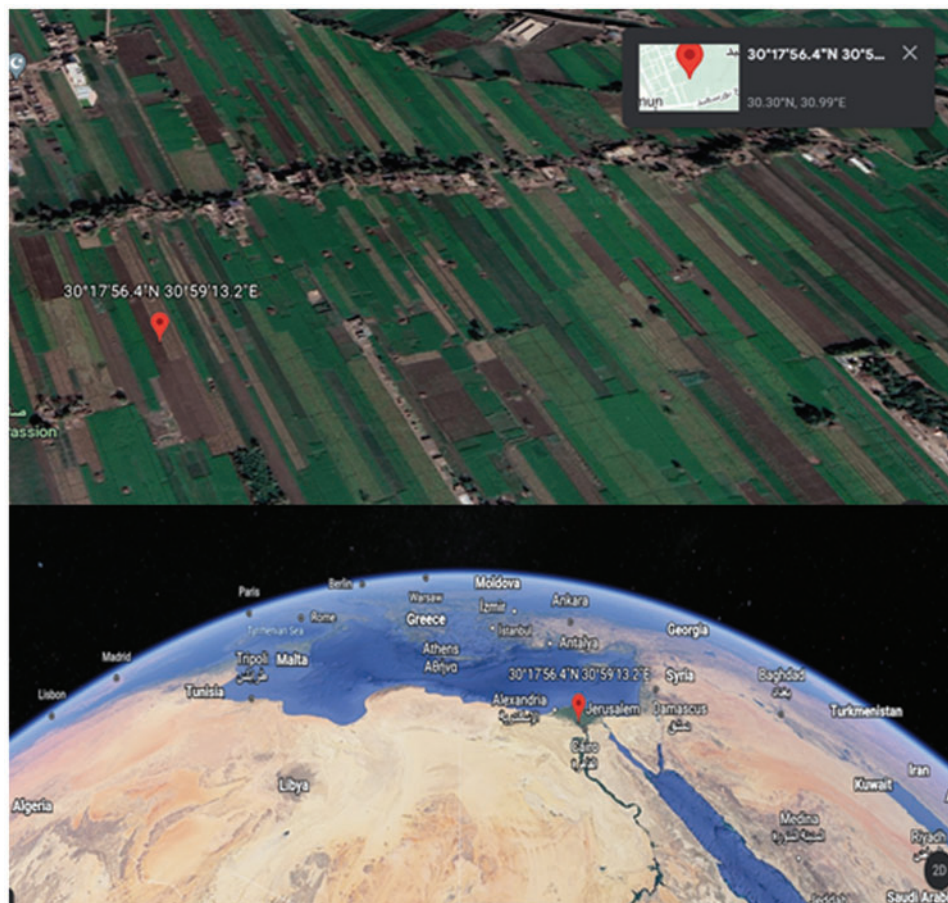


**Figure 1:** Location of the studied system in Ashmon, Egypt

The methods which are used in this analysis will consist of 3 modeling stages. The output data from the first and second stages will be the input data for the next level or stage. The result used in these models will be validated by comparison. The comparison will be with either analytical results (from an approved research paper), or empirically (measured data in approved research papers). The first stage of modeling will be related to Irradiance models and Irradiance data sources for long-term analysis, PVGIS satellite Irradiance data TMY-(Typical Meteorological Year) will be used. This data has a very good accuracy compared to calibrated verified and checked ground weather stations around the world (Baseline Surface Radiation Network (BSRN)) [28] which are used by PVGIS. This data will be adjusted and conditioned in a format to be accepted and processed by MATLAB-coded programs. TMY data that will be used lies in the epoch from the year 2007 to 2016. The raw data will be fed to the model including DNI, DHI, and GHI Insolation data. In this work we will use two Irradiance models:

1. Lui and Jordan Isotropic Irradiance Model [10,11].
2. Hay and Davies circumsolar Irradiance Model [13].

The output of these irradiance models will suffer from the air mass effect. To consider such an effect, we will use the airmass modifier calculations [29], and  $G_{mtot}$ , which will be total irradiance in-plan radiation. However, the constants are used in the AM modifier related to monocrystalline technology, but de Soto et al. [29] declared that if it is used for polycrystalline technology, the results will cause a minimal error which could be ignored. A validation of this stage will be conducted by comparing the output of our simulation and PVGIS total radiation estimated in one-year period of time. Total insolation which will fall on the modules will be converted to DC electric power by the solar cells in the modules. A model is needed to simulate the power generation and the behavior of these cells. One of the most well-known models is the one diode model or 5 parameters model. The dilemma of these models is to determine the 5 parameters to make the generated voltage and current of the cell identical to those in the datasheet of the manufacturer under STC conditions. In this paper we will use the analytical model, [30], along with iterative calculations using MATLAB coding to determine the 5 parameters (Ideality factor of the diode  $n$ , Photon current  $I_{ph}$ , Saturation current  $I_0$ , Series resistance  $R_s$ , Shunt resistance  $R_{sh}$  or  $(R_p)$ , Thermal voltage  $V_t$ ) validation will be conducted by comparing the output of the cell with empirically measured results of the Shell Solar SQ175-PC PV module Ma et al. [30]. Although in the previous section the output of the module is compared to empirically measured data, it does not reflect the behavior of the solar generator on long-term analysis, so the validated solar cell model will be fed with TMY total irradiance data for one year [28]. The output of the system will be compared to the same system simulated by the European site PVGIS to determine the accuracy and validation of the system model in working environmental conditions.

## 2.1 Irradiance Models (Level 1 Algorithm)

The irradiance model utilized in this work will be the Isotropic Irradiance Model, the Hay and Davis model, along with the air mass modifier.

### 2.1.1 Isotropic Irradiance Model

Using Lui and Jordan Isotropic Irradiance model [10,11]. As following sets of equations:

$$a_M = 90^\circ - \theta_M \quad (1)$$

$$G_M^{tot} = G_M^{dir} + G_M^{dif} + G_M^{alb} \quad (2)$$

$$G_M^{dir} = SF \cdot DNI \cdot \cos(AOI) \quad (3)$$

$$\cos(AOI) = \cos(a_M) \cdot \cos(a_s) \cdot \cos(A_M - A_s) + \sin(a_M) \cdot \sin(a_s) \quad (4)$$

$$G_M^{dif} = SVF \cdot DHI \quad (5)$$

$$SVF = \frac{1 + \cos(\theta_M)}{2} \quad (6)$$

$$G_M^{alb} = \alpha_{gnd} \cdot (1 - SVF) \cdot GHI \quad (7)$$

$$AOI = \angle(A_M, a_M)(A_s, a_s) \quad (8)$$

where:

$A_M$	Is Module azimuth [°].
$A_s$	Is Sun azimuth [°].
$a_M$	Is Module altitude [°].

$A_s$	Is Sun altitude [ $^\circ$ ].
$G_M^{\text{tot}}$	Total irradiance on square meter of the panel [ $\text{W}/\text{m}^2$ ].
$G_M^{\text{dir}}$	Is the direct normal irradiance [ $\text{W}/\text{m}^2$ ].
$G_M^{\text{dif}}$	Is the diffused irradiance [ $\text{W}/\text{m}^2$ ].
SVF	Sky view factor.
DHI	Diffuse horizontal irradiance [ $\text{W}/\text{m}^2$ ].
$G_M^{\text{alb}}$	Albedo irradiance [ $\text{W}/\text{m}^2$ ].
$\alpha_{\text{gnd}}$	Is the albedo coefficient.
GHI	Is the global horizontal irradiance [ $\text{W}/\text{m}^2$ ].
$\theta_M$	Is module tilt angel in degrees [ $^\circ$ ].
$(\theta_z)$	or AOI Is the angle of incidence [ $^\circ$ ].

Figs. 2 and 3 show the trigonometry which is used to calculate angle of incidence [31].

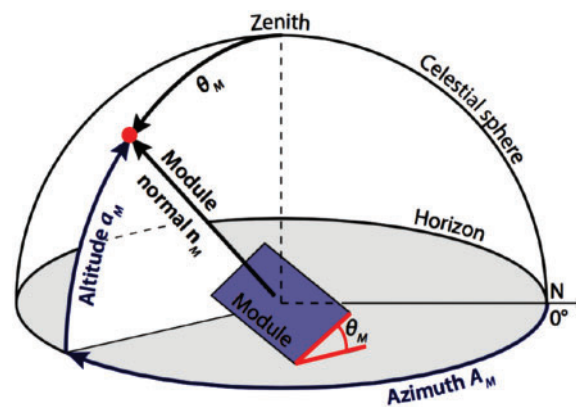


**Figure 2:** Different angles to determine (AOI) angle of incidence

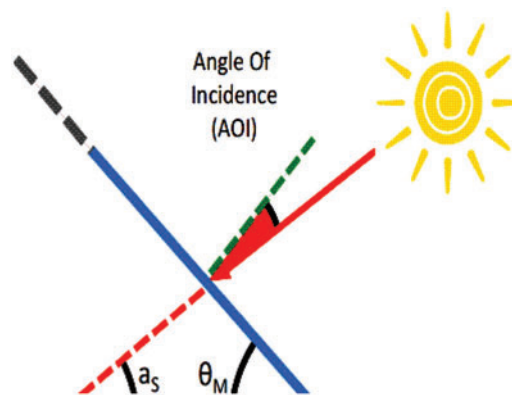


**Figure 3:** Definition of AOI

In above model the diffuse irradiance is isotopically distributed in the earth's atmosphere. No circumsolar ring around the sun is considered or horizon brightening components.



### 2.1.2 Hay and Davies Anisotropic Irradiance Model Equation

As stated by Hay [13], they calculate monthly mean solar radiation for horizontal and inclined surfaces Using following set of equations:

$$G_M^{\text{tot}} = \left( \text{DNI} + \text{DHI} \cdot \frac{\text{DNI}}{\text{DNI}_{\text{EX}}} \right) \cdot \text{SF} \cdot \cos(\text{AOI}) + \text{DHI} \cdot \left( 1 - \frac{\text{DNI}}{\text{DNI}_{\text{EX}}} \right) \cdot \text{SVF} + \alpha_{\text{gnd}} \cdot (1 - \text{SVF}) \cdot \text{GHI}.$$

$$\text{DNI}_{\text{EX}} = S \cdot \left( \frac{R_{\text{av}}}{R} \right)^2. \quad (10)$$

where:

$\text{DNI}_{\text{EX}}$	Extraterrestrial direct normal irradiance on horizontal plan Empirical formula [ $\text{W}/\text{m}^2$ ].
$S$	Extraterrestrial radiation on horizontal plan [ $\text{Wh}/\text{m}^2$ ].
$R_{\text{av}}$	Average sun-Earth distance [m].
$R$	Actual sun-Earth distance [m].
$\text{DNI}$	Direct normal irradiance hourly basis [ $\text{W}/\text{m}^2$ ].
$\text{DHI}$	Diffuse horizontal irradiance hourly basis [ $\text{W}/\text{m}^2$ ].
$\text{SF}$	Shading factor.
$\text{SVF}$	Sky view factor.

In this method diffuse Irradiation is considered to be composed of 2 components:

- Isotropic diffuse irradiance.
- circumsolar diffuse irradiance.

### 2.1.3 Airmass Modifier

Airmass (AM) is defined as the mass of atmosphere above Earth in which the light will travel and suffering of dispersion and spectral distribution according to the wave length of the components [32, 29, 33].

$$G_{\text{M-AM}}^{\text{tot}}(i) = M(i) \times (G_{\text{M}}^{\text{dir}}(i) + G_{\text{M}}^{\text{dif}}(i) + G_{\text{M}}^{\text{alb}}(i)) \quad (11)$$

where:

$M(i)$ : the Airmass Modifier.

$i$ : hourly index of the Airmass Modifier.

$G_{\text{M-AM}}^{\text{tot}}(i)$  Total Irradiance on Module affected by airmass modifier [ $\text{W}/\text{m}^2$ ].

$$M = \sum_{j=0}^4 a_{\text{am},j} (\text{AM})^j \quad (12)$$

$$M = 0.935823 + 0.054289(\text{AM}) - 0.008677(\text{AM})^2 + 0.000527(\text{AM})^3 - 0.000011(\text{AM})^4. \quad (13)$$

$a_{\text{am},j}$ : a string of constants

$$\text{AM} = \frac{1}{\cos(\theta_z)} \quad (14)$$

## 2.2 Solar Cell (One Diode) 5 Parameters Model (Level 2 Algorithm)

Cubas et al. [24] proposed a set of equations which determine the values of the solar cell/panel 5 parameters as shown in Fig. 4, Javier used the following boundary equations accompanied with some simplifications. Accuracy of the values is very near or better than accuracy determined by other methods. Boundary conditions and their equations are:

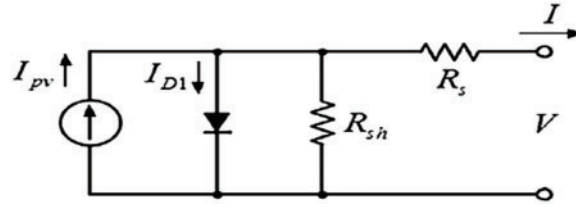


**Figure 4:** One diode 5 parameters solar cell model

(1) One diode 5 parameters solar cell model equation:

$$I = I_{pv} - I_0 \left[ \exp \left( \frac{V + IR_s}{aV_T} \right) - 1 \right] - \frac{V + IR_s}{R_{sh}}. \quad (15)$$

(2) Short circuit boundary condition:

$$I_{SC} = I_{pv} - I_0 \left[ \exp \left( \frac{I_{SC}R_s}{aV_T} \right) - 1 \right] - \frac{I_{SC}R_s}{R_{sh}} \quad (16)$$

(3) Open circuit boundary condition:

$$0 = I_{pv} - I_0 \left[ \exp \left( \frac{V_{oc}}{aV_T} \right) - 1 \right] - \frac{V_{oc}}{R_{sh}}. \quad (17)$$

(4) Maximum power point differentiation condition:

$$\left( \frac{\partial I}{\partial V} \right) \Big|_{[I_{mp}, V_{mp}]} = - \frac{I_{mp}}{V_{mp}}. \quad (18)$$

where:

$I$	Solar cell total current [A].
$I_{pv}$	Photo voltaic generated current [A].
$I_0$	Diode saturation current [A].
$V_T$	Thermal voltage of the diode [V].
$a$	Ideality factor of the solar cell.
$I_{SC}$	Short circuit current of the solar cell [A].
$V_{oc}$	Open circuit voltage of the solar cell [V].
$R_s$	Series resistance of the solar cell [ $\Omega$ ].
$R_{sh}$	Shunt resistance of the solar cell [ $\Omega$ ].

An implicit expression of the series resistor,  $R_s$ , as a function of the initial known parameters:

$$\frac{aV_T V_{mp} (2I_{mp} - I_{SC})}{(V_{mp} I_{SC} + V_{oc} (I_{mp} - I_{SC})) (V_{mp} - I_{mp} R_s) - aV_T (V_{mp} I_{SC} - V_{oc} I_{mp})} = \exp \left( \frac{V_{mp} + I_{mp} R_s - V_{oc}}{aV_T} \right) \quad (19)$$

Final expression of the shunt resistor,  $R_{sh}$ , as a function of  $R_s$  and the initial parameters:

$$R_{sh} = \frac{(V_{mp} - I_{mp} R_s) (V_{mp} - R_s (I_{SC} - I_{mp}) - aV_T)}{(V_{mp} - I_{mp} R_s) (I_{SC} - I_{mp}) - aV_T I_{mp}} \quad (20)$$

where:

- $V_{mp}$  Maximum power point voltage [V].
- $I_{mp}$  Maximum power point current [A].

These equations are validated by applying the methodology and iterative algorithm suggested by Zekry et al. [25], to determine the values of the 5 parameters:

1. Initiating a value for ideality factor (a) from 1 to 1.5, increasing by 0.1 each time.
2. Solving symbolic Equation for series resistance using MATLAB coding program.
3. Solving symbolic equations for shunt resistance using MATLAB coded program.
4. Apply all values to MPP and use the data sheet of the manufacturer to get the best estimation of the parameters. The results were compared to Ma et al. [30], using shell SQ175-PC solar cell at STC conditions. Excellent matches were found in key points in the I-V and I-P curves. After solving the symbolic equations and getting accepted values for parameters in STC, the photon current equations are fed by Irradiance model output data to determine the generated power of the solar generator throughout the year in an hourly, daily, monthly, and yearly manner. In this paper we used a set of equations suggested by Zekry et al. [25] to simulate working solar panels in different environmental working conditions.

### 2.3 Solar Generator Model including Cables/Inverter Losses (Level 3 Algorithm)

Based on Zekry et al. model [25], the following set of equations to simulate behavior of solar cell/panel in working conditions:

$$I = I_{ph} - I_s \left( e^{\frac{q(V+IR_s)}{nk_B T}} - 1 \right) - \frac{V + IR_s}{R_{sh}} \quad (21)$$

$$I = I_{ph} - I_s \left( e^{\frac{q(V+IR_s)}{nk_B T}} - 1 \right) - \frac{V + IR_s}{R_{sh}} \quad (22)$$

$$I_{ph(STC)} = I_{SC(STC)} \left( \frac{G}{G_{STC}} \right) \quad (23)$$

$$V_{OC} = V_{OC(STC)} + K_V (T - T_{STC}) \quad (24)$$

$$I_s = I_{s(STC)} \left( \frac{T}{T_{STC}} \right)^3 e^{\frac{-qE_g}{nk_B} \left( \frac{1}{T} - \frac{1}{T_{STC}} \right)} \quad (25)$$

$$I_s (STC) = \frac{I_{SC(STC)}}{\left( e^{\frac{qV_{OC(STC)}}{nk_B T_{STC}}} - 1 \right)} \quad (26)$$

where:  $E_g$  is the band gap energy of the semiconductor [eV];  $G$  is the surface irradiance of the cell [ $W/m^2$ ];  $G_{STC}$  is the irradiance under STC ( $T = 25^\circ C$  and  $P = 1000 W/m^2$ );  $I_{s(STC)}$  is the nominal saturation current [A];  $I_{SC(STC)}$  is the short circuit current per cell at STC [A];  $k_B$  is the Boltzmann's constant [ $J \cdot K^{-1}$ ];  $K_I$  is the temperature coefficient of short circuit current [ $\%/^\circ C$ ];  $K_V$  is the temperature coefficient of open-circuit voltage [ $\%/^\circ C$ ];  $n$  is the diode ideality factor; STC is standard test conditions at which ( $T_{STC} = 25^\circ C$ );  $T$  is the absolute temperature in Kelvin [K]. The output power

generated hourly will be fed to cables and inverter, for simplicity, the losses must be included in the system of equations by simply multiplying the maximum output power  $P_{\max}$  by  $0.97 \times 0.97$  to account of the 3 percent loss for both cabling and inverter.

## 2.4 Simulation and General Block Diagram of System Architecture

As shown in Fig. 5. The algorithm is composed of 3 layers or levels of calculations and models. Each of them is to predict and evaluate certain parts of the whole simulation system. The accuracy and results of each layer of processing depends on the previous layer's results and accuracy, so each level is validated separately. The final generated power (level 3) accounted for the whole system's performance.

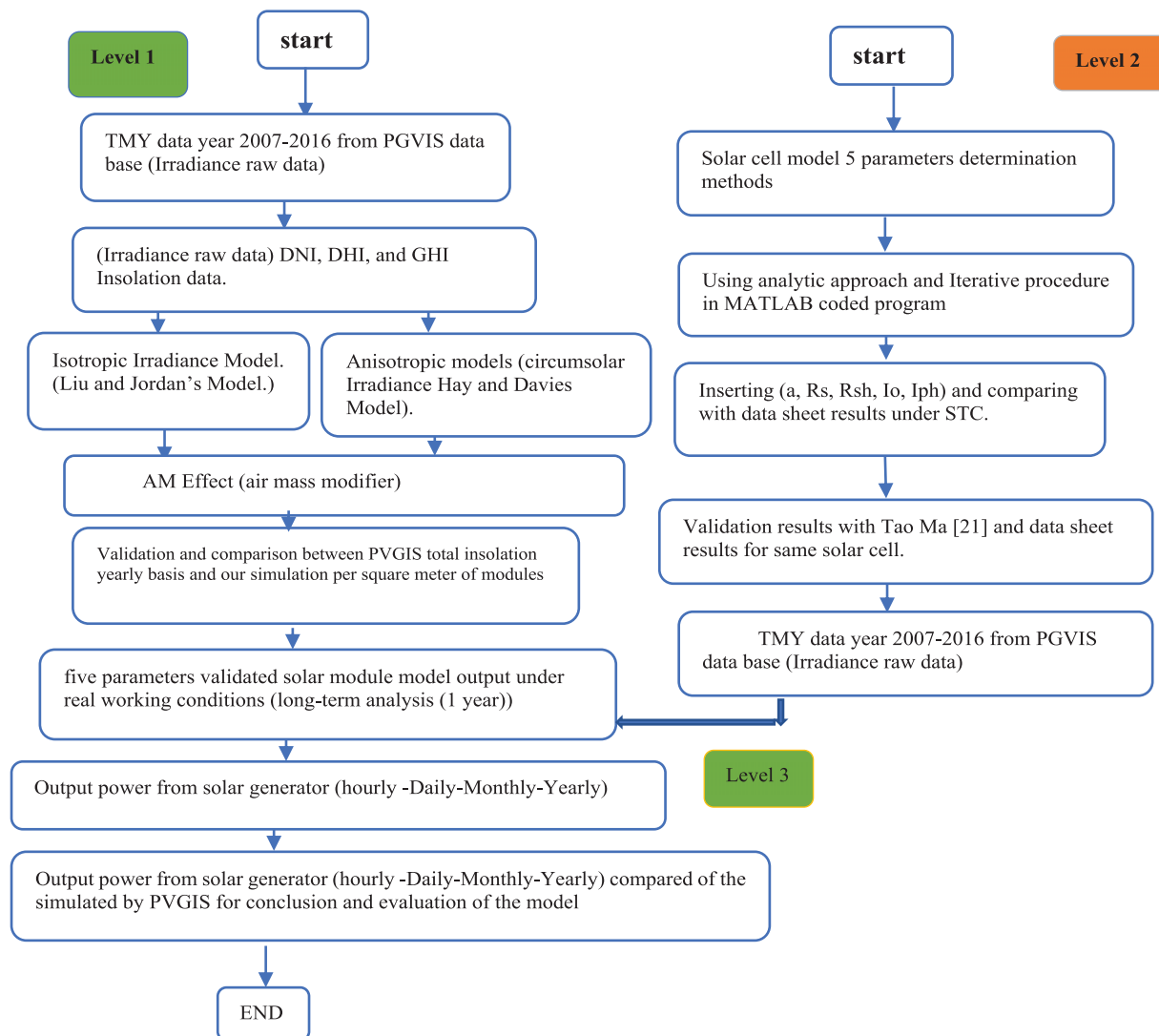
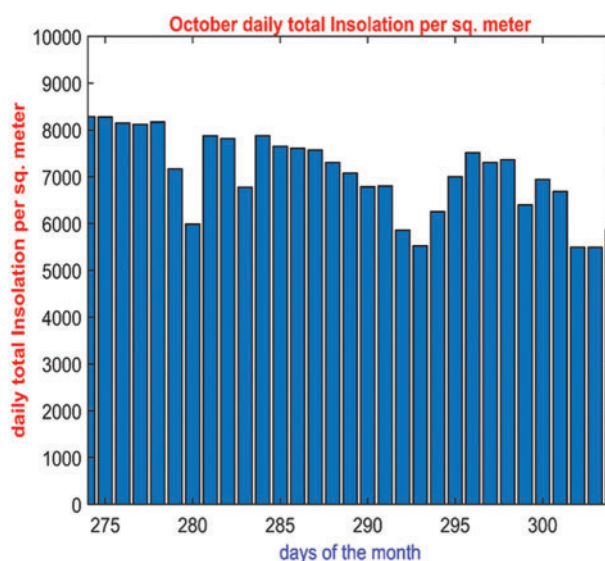


**Figure 5:** Solar generator simulation algorithm in egyptian environment Ashmon/Monofya (Delta of Nile River)

### 3 Simulation Results and Discussion

#### 3.1 Irradiance Model Validation, Results and Discussion (Level 1)

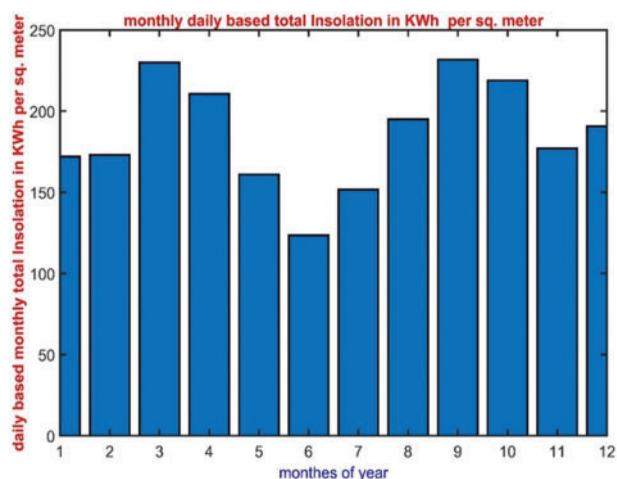
As we stated on section two, we use both types of models isotropic and Anisotropic Models we choose Lui and Jordan Isotropic Irradiance Model, Hay and Davies. The calculations based on 8760 data point entry per year (TMY 2007–2016). The results will output total 8760 hourly total insolation power in plan radiation. This data is integrated into daily, monthly and yearly results and compared with the total in plan insolation depicted by PVGIS European data tool for year 2016. The later (PVGIS) calculated incident power per square meter is 2282.1 KW/m<sup>2</sup> for year 2016, and 2377.579 KW/m<sup>2</sup> for year 2020, while incident power per square meter using proposed system, TMY data (incident power on horizontal plan TMY 2007–2016) simulated by isotropic model and anisotropic model are: 2163.1 and 2160.1 KW/m<sup>2</sup>, respectively. Percentage difference PVGIS results year 2016 and Simulation is about 5.6477% and 5.5039% consecutively. While for 2020 percentage difference PVGIS results and Simulation is about 9.11% and 9.02% consecutively. Also, we notice deviation in incident power per square meter in plan radiation between year 2016 (proposed system) and 2020 (PVGIS) about 4.02% increasing. Fig. 6 shows the daily insolation incident energy in Wh per square meter daily, these values are calculated using Hay and Davis model and by using PVGIS TMY 2009–2016 irradiance data.



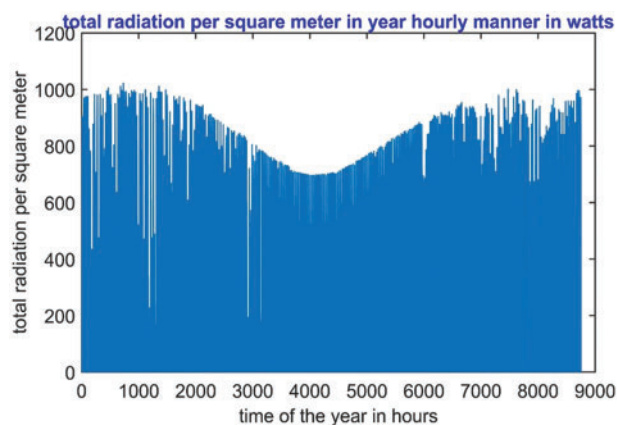
**Figure 6:** October total daily insolation power in KWh/m<sup>2</sup>

Fig. 7 shows the average daily insolation in KWh each month, this is created by summation of insolation all days per month and divide result by days of the month. This is considered an indicator of the daily average insolation in that month.

Fig. 8 shows Total radiation power incident from the sun on Earth per sq. meter in watts hourly basis in a year. It consists of 8760 data entry collected from satellite digital imaging analysis. The components of the Irradiance data are processed using 2 irradiance models and Air Modifier equation to represent the effect of air mass of earth atmosphere. Final Results is expressed in the graph below.



**Figure 7:** TMY data monthly average daily based total in plan insolation simulated in KWh/m<sup>2</sup>



**Figure 8:** Total radiation power per sq. meter in watts hourly basis in a year

As Example of solar yield monthly, [Fig. 9](#) shows total solar insolation for January in Wh per square meter. It is noticed that during winter season the insolation decrease consequently yield energy from the system decrease compared to summer season daily average insolation through the month is 5.6127 KWh. Next [Fig. 10](#) shows total and average solar insolation per square meter in Ashmon daily basis. It is noticed that the average total insolation around the year in this governorate in Egypt is 6.5539 KWh daily.



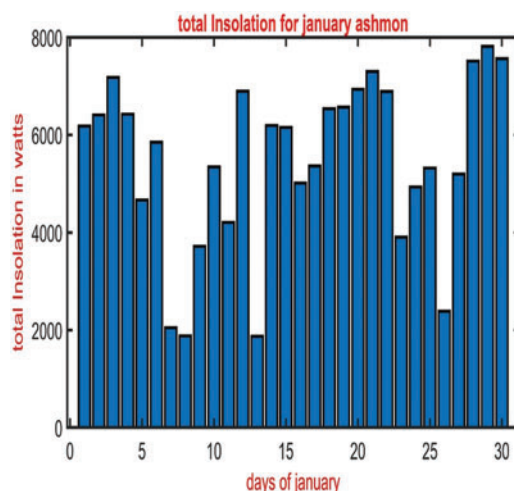


**Figure 9:** Total solar insolation for January in Wh/m<sup>2</sup>

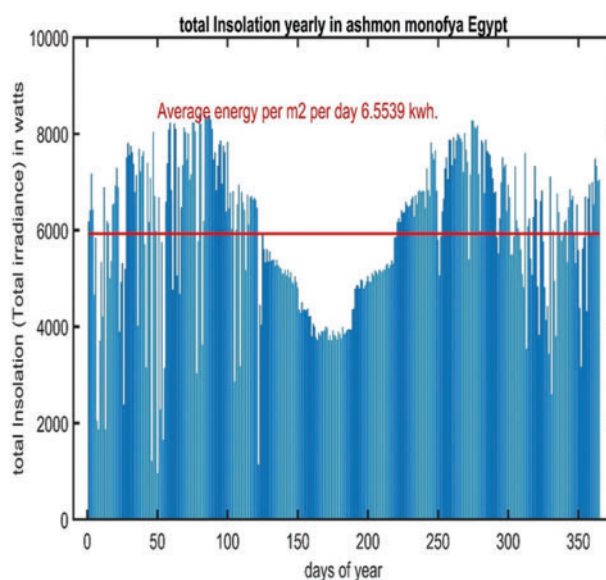


**Figure 10:** Total and average solar insolation per square meter in Ashmon

### 3.2 One Diode Solar Cell Model 5 Parameter Extraction and Validation under STC

As stated in [Section 2](#) the 5 parameters model has decent accuracy and good representation of solar panel in various working conditions. We use the set of equations used by Javier Cubas, in an iterative process executed through MATLAB coding program to determine best fit ideality factor that validate output of the solar cell under STC identical or very near to data sheet results depicted by the manufacturer tests. The key specifications of the Shell Solar SQ175-PC PV module are clarified in [Table 1](#), results of study done by Tao Ma were compared to results in this study. The important points in both I-V and I-P curves almost identical in both analyses.

**Table 1:** The key specifications of the Shell Solar SQ175-PC PV module

Characteristics	Value
Open-Circuit Voltage ( $V_{oc}$ )	44.6 V
Voltage at maximum power point ( $V_{mp}$ )	35.4 V
Short-Circuit Current ( $I_{sc}$ )	5.43 A
Current at maximum power point ( $I_{mp}$ )	4.95 A
Maximum power at STC ( $P_{max}$ ) 175 $W_p$	175 w
Number of cells connected in series	72
Temperature coefficient of $I_{sc}$ (alpha)	0.8 mA/°C
Temperature coefficient of $V_{oc}$ (beta)	145 mV/°C
Temperature coefficient of $P_{mpp}$ (gamma)	0.43%/°C

Fig. 11 shows simulated voltage vs. current with fixed irradiance and varying temperature from 10 C to 70 C degree, it is almost identical to experimentally test done by factory which proof excellent estimation of ideality factor done in this paper approach. Figs. 12 and 13 show simulated output power of the panel with varying temperatures/fixed power and varying incident power/fixed temperature operational conditions, respectively.

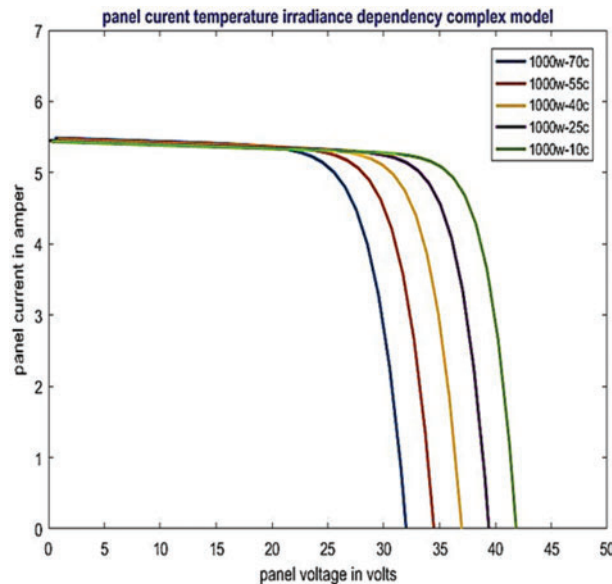
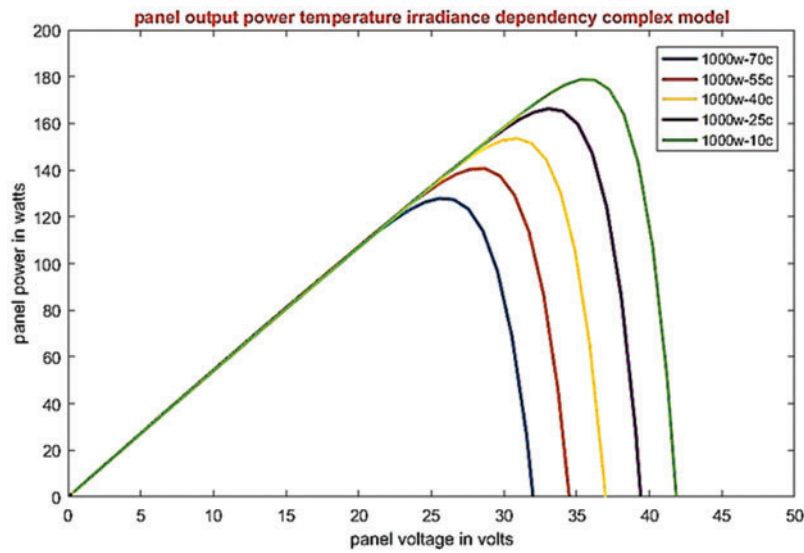
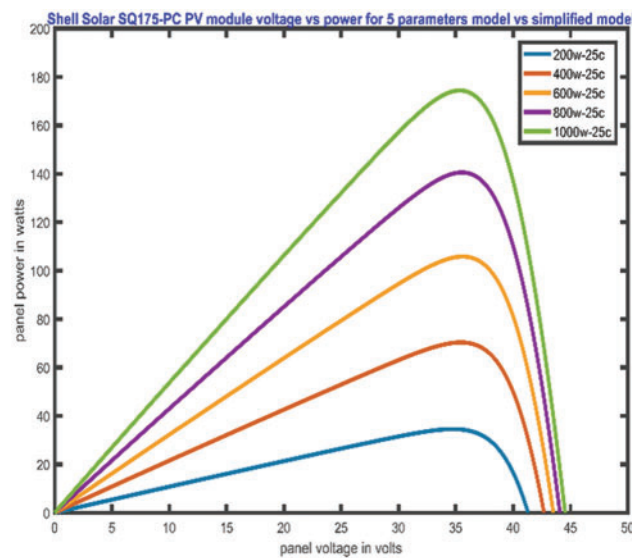
**Figure 11:** Fixed temperature and different irradiance open circuit voltage vs. short circuit current

Fig. 12 shows output power of the panel illuminated with fixed illumination power 1000 watt and varying temperatures. It is noted that max power point dropped almost 30% due to temperature increasing. While in Fig. 13 the temperature is fixed, and Irradiance power is varying, the output of the panel dropped accordingly.



**Figure 12:** Fixed irradiance energy and varying temperature varying power output of panel



**Figure 13:** Fixed temperature and different irradiance panel output

As shown in Table 2 although the values of the parameters are different, but the governing points in the I-V curve and I-P curve were almost identical to results of mentioned paper [32] Tao Ma under STC.

**Table 2:** Calculated parameters of PV cell/module vs. Tao Ma results

Cell parameter	$I_{ph}$	$I_0$	$R_s$	$R_{sh}$ or ( $R_b$ )	$V_t$	$n$
Tao Ma results	5.449	1.20E-09	0.010	2.725	0.028	1.086
This work results	5.4493	1.30E-09	0.0097	2.7354	0.02567	1.09

### 3.3 Five Parameter Model Solar Panel Output vs. Simplified Model Ignoring $R_s$ Compared to $R_{sh}$ ( $(R_s <<)$ and $(R_{sh} >>)$ )

Here we consider the term  $((I * R_s / R_{sh}) <<)$  and would be neglected, on the other hand we will keep the term  $I * R_s$  in the exponential diode current term. this new arrangement of equation will ignore the whole shunt current in the solar cell and will show the increase of the cell power as a simplified model. Eq. (18) which describes the output current from the cell, will turn to be in the following form

$$I = I_{ph} - I_s \left( e^{\frac{q(V + IR_s)}{nk_B T}} - 1 \right) \quad (27)$$

The used panel used for this analysis is SUNTECH poly crystalline panel STP275-20/Wfw with following Electrical Characteristics as shown in Table 3:

**Table 3:** Electrical Characteristics STC STP275-20/Wfw

Maximum Power at STC ( $P_{max}$ )	275 W
Optimum Operating Voltage ( $V_{mp}$ )	31.2 V
Optimum Operating Current ( $I_{mp}$ )	8.82 A
Open Circuit Voltage ( $V_{oc}$ )	38.1 V
Short Circuit Current ( $I_{sc}$ )	9.27 A
Module Efficiency	16.8%
Operating Module Temperature	-40°C to +85°C
Maximum System Voltage	1000 V DC (IEC)
Maximum Series Fuse Rating	20 A
Power Tolerance	0/+5 W

The following Figs. 14 and 15 show the output raising in current and power due to neglect of Shunt current on the panel output. We notice that at the knee of power curve (i.e., the maximum power point) the neglect of the shunt current increase the total current output of the cell and consequently increases the output power of the cell. The dotted line represents the output power of neglected shunt current cell while the solid line represents the cell which is affected by shunt resistance and shunt current (5 parameters solar cell full model). The same effect could be noticed on the V-I curve, at the  $V_{mpp}$  (voltage at maximum power point) a considerable raise in current due to ignoring the current flow in the shunt branch as shown in Fig. 16.

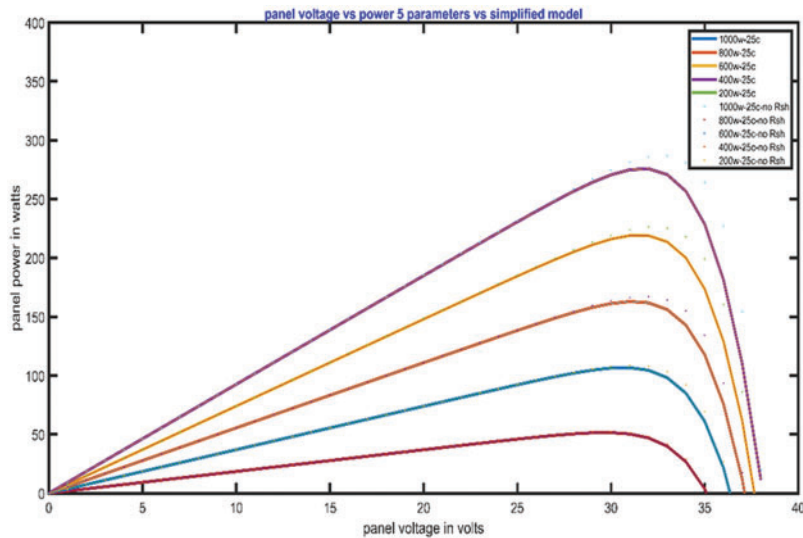


**Figure 14:** Const temperature simplified (dotted) vs. complex model, voltage current output

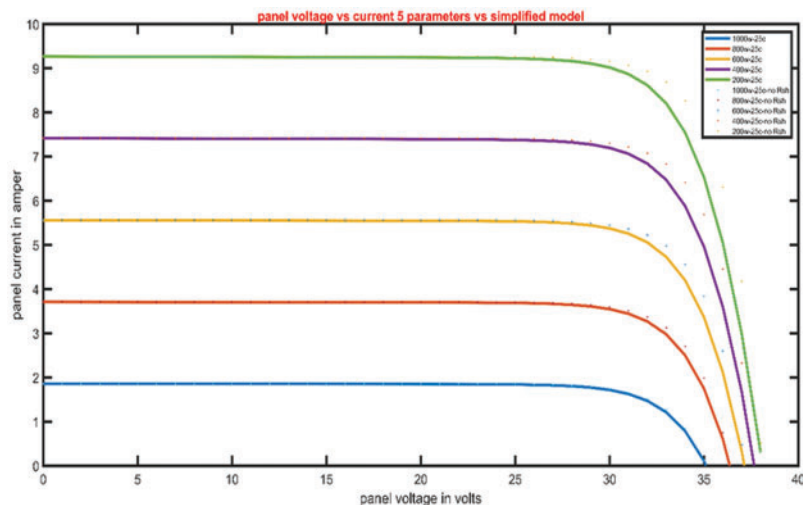


**Figure 15:** Const temperature simplified (dotted) vs. complex model power curve

Until this point in the article we only tested the solar cell/panel/array in lab conditions only. That we use insolation power with in controlled conditions to feed and test the model. These conditions do not reflect environmental working daily conditions. In the next section we will start feeding the model with all predicted data based on satellite imagery system in hourly basis to analyze and predict the real performance of these systems in several applications. This will allow us to know limitations of these systems in daily life use and reliability of solar stand-alone systems or on-grid systems for certain application. The motivation of this model is to merge it in future work in solar pumping irrigation system to test ability of solar system in agricultural sector as stand-alone systems. Also, another prospective will be studied the effect of using these systems in the economy of developing countries, which suffering from energy problems.

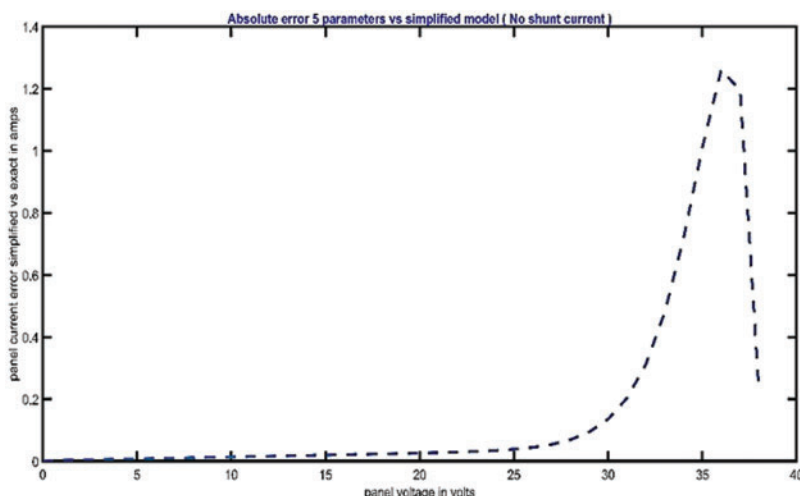


**Figure 16:** Absolute error in power generation between simplified vs. complex model

### 3.4 Five Parameters Validated Solar Module Model Output under Real Working Conditions (Long-Term Analysis (1 Year))

Based on Zekry model, we use the equations stated above to represent the solar array, and fed the solar generator with TMY irradiation data from years 2007 to 2016 in hourly basis, after conditioning and preparing the data to the suitable format, we deduce the in-plan radiation and apply airmass modifier to it, furthermore, the losses due to inverter and cables are considered, then the total generated power is compared to the generated power simulated by PVGIS European web site (JRC tools). This model (PVGIS) is based on Muneer model. And radiation data of year 2022. We found that the total generated power by PVGIS model was 14828.71 KWh per year for the nominal power of 8.25 KW<sub>p</sub> system on the other hand the same nominal power of the system simulated in this work, gives yield of 13644.33 KWh per year the ratio between the two system was found to be 92% as following equation:

$$\text{ratio} = \frac{\text{pcomplex\_PVGIS\_results}}{\text{simulated\_pcomplex\_after\_losses\_inverter\_cables\_sum}}$$

i.e., the simulation increased output is more than the PVGIS output by 8%. Although the years used in this analysis was TMY data from years 2007 to 2016. And PVGIS data for year 2022.

Figs. 17 and 18 show energy yield yearly normalized to 1 KW<sub>p</sub> (Kilo Watt peak system) in hourly and monthly basis respectively. It is worth mentioning that yield energy in winter months (1,2,11,12) are less than summer season (6,7,8,9). While Table 4 shows simulated energy yield for each month using proposed models in this paper. The hourly irradiance data extracted from PVGIS TMY data base. It is conditioned and processed to generate hourly basis energy yield of normalized 1 KW<sub>p</sub> system.

In next Figs. 19 and 20 a system of 8.25 KW<sub>p</sub> is taken as a case study for data analysis. It shows final yield simulated by PVGIS platform (of European union) and yield of the same system (8.25 KW<sub>p</sub> system) simulated by proposed approach. These results are summarized in Table 5.



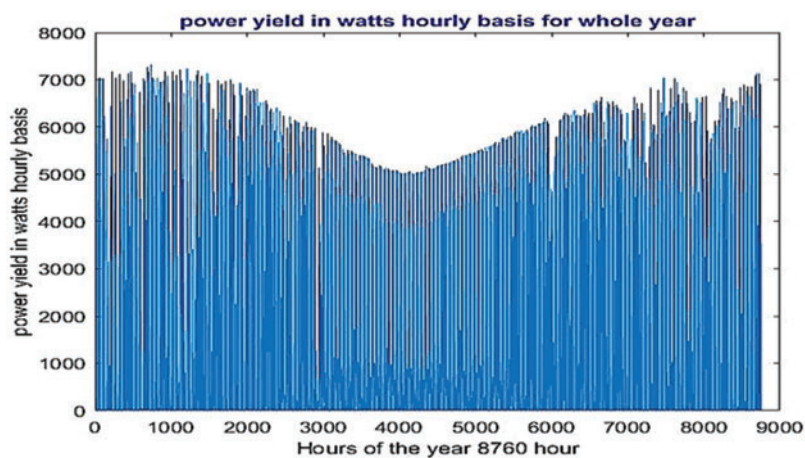


**Figure 17:** Power yield in watts hourly basis for whole year

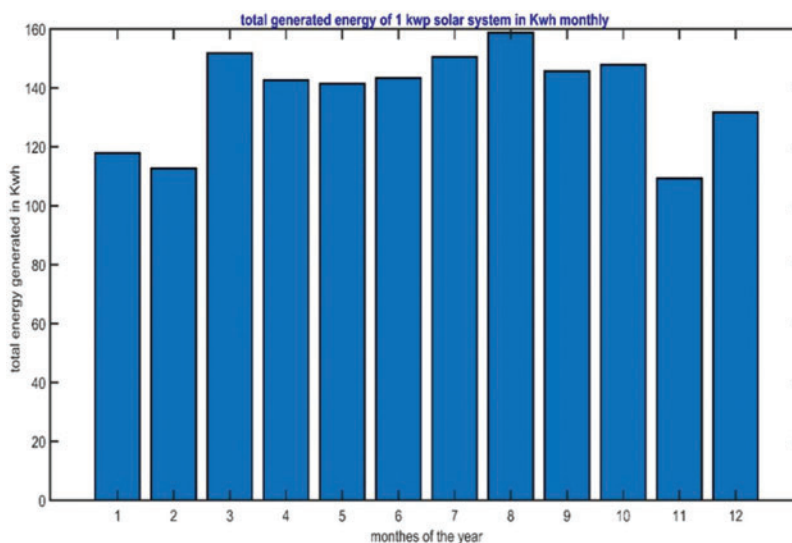


**Figure 18:** Monthly energy output for 1 KW<sub>p</sub> system simulated in this work

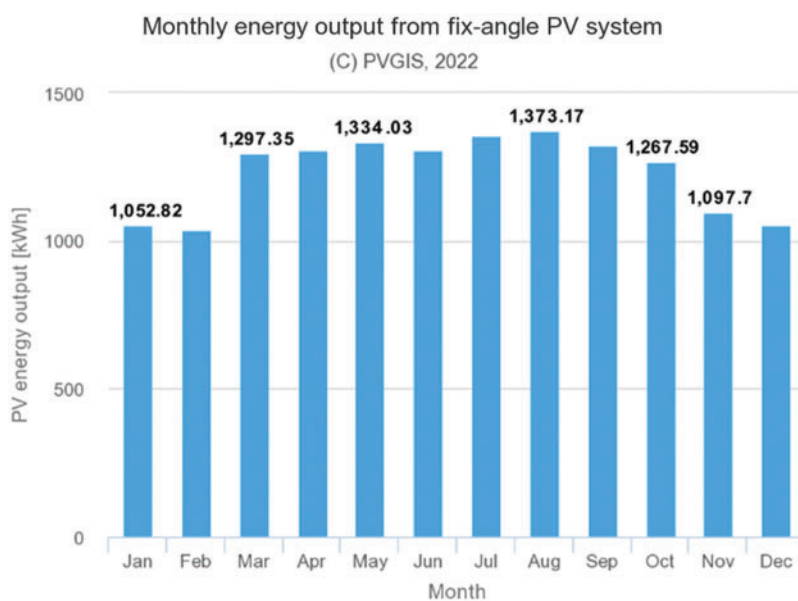
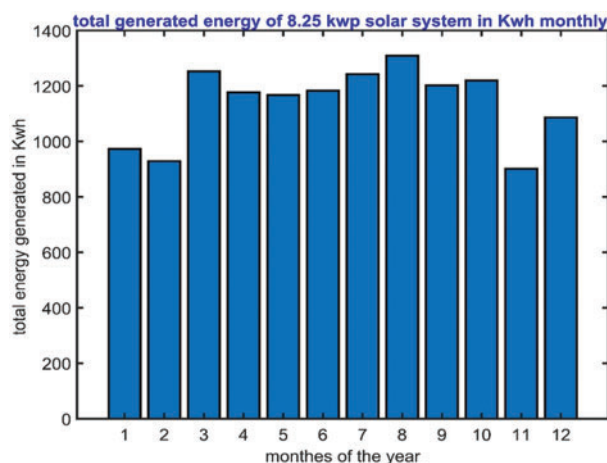
**Table 4:** Daily average energy monthly basis in KWh

Month	Generated energy in KWh for 1 KW <sub>p</sub> system monthly
January	117.9052
February	112.635
March	151.8479
April	142.6993
May	141.458
June	143.4121
July	150.565

(Continued)

**Table 4 (continued)**

Month	Generated energy in KWh for 1 KW <sub>p</sub> system monthly
August	158.7076
September	145.6952
October	147.9126
November	109.3154
December	131.7055

**Figure 19:** Monthly energy output PVGIS simulation system**Figure 20:** Monthly energy output for 8.25 KW<sub>p</sub> system simulated in this work

**Table 5:** Monthly generated energy from PVGIS and simulated system in this work

System used	Simulated	PVGIS	Ratio
Units	KWh	KWh	Ratio %
January	972.7183	1052.82	92.392%
February	929.2385	1042	89.178%
March	1252.745	1297.35	96.562%
April	1177.269	1307.35	90.050%
May	1167.028	1334.03	87.481%
June	1183.15	1323	89.429%
July	1242.161	1373.17	90.459%
August	1309.338	1370	95.572%
September	1201.985	1272	94.496%
October	1220.279	1267.59	96.268%
November	901.8519	1097.7	82.158%
December	1086.57	1091.7	99.530%
Total	13644.33	14828.71	92.013%

#### 4 Conclusions

In this paper we tried to explain a method to practically evaluate the output of PV generator depending on available radiation data on the internet network for free, this method use sets of models for each level starting from irradiance data processing to solar parameter extraction and long term energy yield, using available TMY data from PVGIS website, although the raw data available ending in year 2016, the generated output power (solar energy yield) simulated, compared to the calculated energy yield in year 2022 was very near 8% difference (taking in consideration aging factor loss of efficiency 20 percent in 20 years), this tool could be used as a whole system simulator to accurately calculate the energy generated from PV solar water pumping system or any other system without any need to use paid tools or programs. Through coding the stated equations above in MATLAB programming language. And using the flow chart explained in details second step is to insert the TMY data, and some iterating procedure, the goal is to extract the solar cell 5 unknown parameters, then use the solar cell model in simulating program fed by climate data. The final results turned to be decently accurate, moreover if the available weather data is more recent it will reduce the difference between simulated output and PVGIS results. The novelty of this methodology that it uses all models from the very beginning (i.e., integration and testing of all level models under working conditions), Estimating and extracting of solar cell 5 parameters (i.e., 5 parameter model) through long term evaluation of energy yield in daily working conditions to design and to predict solar system output. Also, a novel method by applying all irradiance data to solar cell equation, this is will lead to get generated current hourly basis, then use current to estimate output power. This tool could be used by engineers to design solar systems and predict its performance in real working conditions. all models could be interchangeably used with different known models to test as many models as required for research. In future work, this model will be merged into solar pumping irrigation system to determine the effect of solar power nature on time sensitive application like agriculture and irrigation. In addition,

the reliability of stand-alone solar pumping irrigation system should be discussed, and lastly feasibility of these system in developing countries like Egypt will be discussed as well. Limitation of this work, that it does not use latest irradiance data to predict exact yield in 2022, as the only available free irradiance data in the available resources is up to year 2016. Also, a 20-year degradation effect is taken in consideration so the actual output is degraded 0.5% each year with total degradation of 10% in the end of 20 year. All paid platforms design and simulate solar generator and upsizing the system to overcome this phenomenon.

**Acknowledgement:** The authors acknowledge the supervising professors, the reviewers, the journal editorial Board, for providing valuable comments and helpful suggestions to improve the manuscript.

**Funding Statement:** The authors received no specific funding for this study.

**Conflicts of Interest:** The authors declare that they have no conflicts of interest to report regarding the present study.

## References

1. Abdelhaleem, F. S., Basiouny, M., Ashour, E., Mahmoud, A. (2021). Application of remote sensing and geographic information systems in irrigation water management under water scarcity conditions in Fayoum, Egypt. *Journal of Environmental Management*, 299(113), 11–36. DOI 10.1016/j.jenvman.2021.113683.
2. Adun, H., Ishaku, H. P., Ogungbemi, A. (2022). Towards Renewable energy targets for the Middle East and North African region: A decarbonization assessment of energy-water nexus. *Journal of Cleaner Production*, 347(3), 133944. DOI 10.1016/j.jclepro.2022.133944.
3. Sontake, V., Kalamkar, V. (2016). Solar photovoltaic water pumping system—A comprehensive review. *Renewable and Sustainable Energy Reviews*, 59(3), 1038–1067. DOI 10.1016/j.rser.2016.01.021.
4. Parvaresh Rizi, A., Ashrafzadeh, A., Ramezani, A. (2019). A financial comparative study of solar and regular irrigation pumps: Case studies in Eastern and Southern Iran. *Renewable Energy*, 138, 1096–1103. DOI 10.1016/j.renene.2019.02.026.
5. Radwan, A., Hongyun, H., Ashraf, A., Mustafa, A. M. (2022). Energy use and energy-related carbon dioxide emissions drivers in Egypt's economy: Focus on the agricultural sector with a structural decomposition analysis. *Energy*, 258, 124821. DOI 10.1016/j.energy.2022.124821.
6. Shouman, E. R. (2017). International and national renewable energy for electricity with optimal cost effective for electricity in Egypt. *Renewable and Sustainable Energy Reviews*, 77, 916–923. DOI 10.1016/j.rser.2016.12.107.
7. Gueymard, C. (1993). Critical analysis and performance assessment of clear sky solar irradiance models using theoretical and measured data. *Solar Energy*, 51(2), 121–138. DOI 10.1016/0038-092X(93)90074-X.
8. Yadav, A. K., Chandel, S. S. (2014). Solar radiation prediction using Artificial Neural Network techniques: A review. *Renewable and Sustainable Energy Reviews*, 33(3), 772–781. DOI 10.1016/j.rser.2013.08.055.
9. Kumar, R., Umanand, L. (2005). Estimation of global radiation using clearness index model for sizing photovoltaic system. *Renewable Energy*, 30(15), 2221–2233. DOI 10.1016/j.renene.2005.02.009.
10. Liu, B., Jordan, R. (1961). Daily insolation on surfaces tilted towards equator. *ASHRAE Journal*, 10, 53–59.
11. Liu, B., Jordan, R. (1960). The interrelationship and characteristic distribution of direct, diffuse and total solar radiation. *Solar Energy*, 4(3), 1–19. DOI 10.1016/0038-092X(60)90062-1.
12. Temps, R., Coulson, K. (1977). Solar radiation incident upon slopes of different orientations. *Solar Energy*, 19(2), 179–184. DOI 10.1016/0038-092X(77)90056-1.
13. Hay, J. (1979). Calculation of monthly mean solar radiation for horizontal and inclined surfaces. *Solar Energy*, 23(4), 301–307. DOI 10.1016/0038-092X(79)90123-3.

14. Reindl, D., Beckman, W., Duffie, J. (1990). Evaluation of hourly tilted surface radiation models. *Solar Energy*, 45(1), 9–17. DOI 10.1016/0038-092X(90)90061-G.
15. Klucher, T. (1979). Evaluation of models to predict insolation on tilted surfaces. *Solar Energy*, 23(2), 111–114. DOI 10.1016/0038-092X(79)90110-5.
16. Perez, R., Stewart, R., Seals, R., Guertin, T. (1988). *The development and verification of the Perez diffuse radiation model*. New York, Albany (USA): Office of Scientific and Technical Information (OSTI).
17. Muneer, T. (1990). Solar radiation model for Europe. *Building Services Engineering Research and Technology*, 11(4), 153–163. DOI 10.1177/014362449001100405.
18. Mousavi Maleki, S., Hizam, H., Gomes, C. (2017). Estimation of hourly, daily and monthly global solar radiation on inclined surfaces: Models re-visited. *Energies*, 10(1), 134. DOI 10.3390/en10010134.
19. Chenni, R., Makhoulouf, M., Kerbache, T., Bouzid, A. (2007). A detailed modeling method for photovoltaic cells. *Energy*, 32(9), 1724–1730. DOI 10.1016/j.energy.2006.12.006.
20. Ma, T., Yang, H., Lu, L. (2014). Solar photovoltaic system modeling and performance prediction. *Renewable and Sustainable Energy Reviews*, 36, 304–315. DOI 10.1016/j.rser.2014.04.057.
21. Ding, J., Radhakrishnan, R. (2008). A new method to determine the optimum load of a real solar cell using the Lambert W-function. *Solar Energy Materials and Solar Cells*, 92(12), 1566–1569. DOI 10.1016/j.solmat.2008.07.004.
22. Cubas, J., Pindado, S., de Manuel, C. (2014). Explicit expressions for solar panel equivalent circuit parameters based on analytical formulation and the Lambert W-function. *Energies*, 7(7), 4098–4115. DOI 10.3390/en7074098.
23. Sera, D., Teodorescu, R., Rodriguez, P. (2007). PV panel model based on datasheet values. *2007 IEEE International Symposium on Industrial Electronics*, pp. 2392–2396. Vigo, Spain. DOI 10.1109/ISIE.2007.4374981.
24. Cubas, J., Pindado, S., Victoria, M. (2014). On the analytical approach for modeling photovoltaic systems behavior. *Journal of Power Sources*, 247, 467–474. DOI 10.1016/j.jpowsour.2013.09.008.
25. Zekry, A., Shaker, A., Salem, M. (2018). Solar cells and arrays: Principles, analysis, and design. *Advances in Renewable Energies and Power Technologies*, 1, 3–56.
26. Sahbel, A., Hassan, N., Abdelhameed, M., Zekry, A. (2013). Experimental performance characterization of photovoltaic modules using DAQ. *Energy Procedia*, 36, 323–332. DOI 10.1016/j.egypro.2013.07.037.
27. Zekry, A., Elgendy, M. (2004). Estimated performance of photovoltaic irrigation systems under different operating conditions. *Twenty-First National Radio Science Conference (NRSC)*, Cairo, Egypt.
28. Huld, T., Müller, R., Gambardella, A. (2012). A new solar radiation database for estimating PV performance in Europe and Africa. *Solar Energy*, 86(6), 1803–1815. DOI 10.1016/j.solener.2012.03.006.
29. De Soto, W., Klein, S., Beckman, W. (2006). Improvement and validation of a model for photovoltaic array performance. *Solar Energy*, 80(1), 78–88. DOI 10.1016/j.solener.2005.06.010.
30. Ma, T., Gu, W., Shen, L., Li, M. (2019). An improved and comprehensive mathematical model for solar photovoltaic modules under real operating conditions. *Solar Energy*, 184(2), 292–304. DOI 10.1016/j.solener.2019.03.089.
31. Smets, A., Jager, K., Isabella, O., van Swaaij, R. (2016). *Solar energy: The physics and engineering of photovoltaic conversion, technologies and systems*. Cambridge, England: UIT Cambridge.
32. King, D., Kratochvil, J., Boyson, W. (2004). *Photovoltaic array performance model*. New York: Sandia National Laboratories, Albuquerque, New Mexico, Livermore, California.
33. Williams, T. (2011). *Optimization of photovoltaic powered deficit irrigation*. Purdue: Purdue University.